New Phytologist

Research

Rhythmic histone acetylation acts in concert with day–night oscillation of the floral volatile metabolic network

Ryan M. Patrick[1,2], **Xing-Qi Huang**[2,3], **Natalia Dudareva**[1,2,3] and **Ying Li**[1,2]

[1]Department of Horticulture and Landscape Architecture, Purdue University, West Lafayette, IN 47907, USA; [2]Purdue Center for Plant Biology, Purdue University, West Lafayette, IN, 47907, USA; [3]Department of Biochemistry, Purdue University, West Lafayette, IN 47907, USA

Author for correspondence:
Ying Li
Email: li2627@purdue.edu

Received: *17 August 2023*
Accepted: *8 November 2023*

New Phytologist (2024) **241:** 1829–1839
doi: 10.1111/nph.19447

Key words: diurnal regulation, histone acetylation, petunia, specialized metabolism, volatile organic compound.

Summary

- The biosynthesis of specialized metabolites is strictly regulated by environmental inputs such as the day–night cycle, but the underlying mechanisms remain elusive. In *Petunia hybrida* cv. Mitchell flowers, the biosynthesis and emission of volatile compounds display a diurnal pattern with a peak in the evening to attract nocturnal pollinators.
- Using petunia flowers as a model system, we found that chromatin level regulation, especially histone acetylation, plays an essential role in mediating the day–night oscillation of the biosynthetic gene network of specialized metabolites.
- By performing time-course chromatin immunoprecipitation assays for histone modifications, we uncovered that a specific group of genes involved in the regulation, biosynthesis, and emission of floral volatile compounds, which displays the greatest magnitude in day–night oscillating gene expression, is associated with highly dynamic histone acetylation marks H3K9ac and H3K27ac. Specifically, the strongest oscillating genes featured a drastic removal of histone acetylation marks at night, potentially to shut down the biosynthesis of floral volatile compounds during the morning when they are not needed. Inhibiting daytime histone acetylation led to a compromised evening induction of these genes.
- Overall, our study suggested an active role of chromatin modification in the diurnal oscillation of specialized metabolic network.

Introduction

Specialized metabolites, also known as secondary metabolites, are crucial for plant fitness and crop production. Plant fitness, defined here as reproductive success over a generation, relies on effective pollination and efficient defense against pathogens and herbivores until seed dispersal. Plants synthesize a wide range of specialized metabolites, including 1700 different volatile organic compounds (VOCs; Knudsen *et al.*, 2006), which play essential roles in facilitating successful interactions with the surrounding environment. Plant VOCs are typically lipophilic low-molecular-weight compounds with high vapor pressure at ambient temperature, which are released from leaves, flowers, and fruits into the atmosphere and from roots into the soil (Dudareva *et al.*, 2013). They play essential roles in attracting pollinators, mediating plant–plant and inter-organ signaling, and protecting plants against biotic or abiotic stresses (Vickers *et al.*, 2009; Holopainen & Gershenzon, 2010). As a result, plant volatiles are essential for crop economy as well as the food industry by contributing to palatability in the latter (Schwab *et al.*, 2008; Klee, 2010).

Over the last two decades, significant progress has been made toward understanding the biosynthesis of plant VOCs, and more recently, the molecular mechanisms involved in their emission. Plant VOCs rely on primary metabolism to provide precursors and energy. Based on the biosynthetic origin, plant VOCs are divided into several classes, including terpenoids, phenylpropanoids/benzenoids, fatty acid derivatives, and amino acid derivatives (Dudareva *et al.*, 2013). For example, the petunia floral VOCs are mainly composed of volatile phenylpropanoid/benzenoid compounds, derived from the aromatic amino acid phenylalanine (Phe) that is produced by the shikimate and Phe biosynthesis pathways (Dudareva *et al.*, 2013). Recently, it has been shown that VOC release from flowers to the atmosphere depends on ABC transporter (ABCG1)-mediated transport across the plasma membrane (Adebesin *et al.*, 2017) and is facilitated by nonspecific lipid transfer proteins across the hydrophilic cell wall (Liao *et al.*, 2023).

The biosynthesis and emission of plant volatiles are species-, organ-, and tissue-specific, developmentally and/or temporally regulated, and responsive to biotic factors such as pollinator interaction and herbivore infestation as well as abiotic factors including temperature, light intensity, atmospheric CO_2, relative humidity, and nutrient status (Verdonk *et al.*, 2003; Colquhoun *et al.*, 2010; Maeda *et al.*, 2010). The floral scent emission often exhibits a rhythmic pattern during a day–night cycle that is synchronized with the foraging activity of the respective pollinators (Verdonk *et al.*, 2003; Fenske *et al.*, 2015). It has been shown that the level of substrate in the cell is involved in the regulation

of rhythmic emission of VOCs (Kolosova *et al.*, 2001). Indeed, the endogenous levels of Phe, the precursor of benzenoid/phenylpropanoid compounds produced by petunia flowers, oscillate during a light/dark cycle and positively correlate with Phe-derived volatile emission peaking at night, when the moth pollinators are most active (Kolosova *et al.*, 2001). Recent studies also revealed that floral VOC biosynthesis is largely regulated at the level of gene expression (Dudareva *et al.*, 2000; Muhlemann *et al.*, 2012). Floral VOC networks are controlled by the circadian clock transcription factor (TF) LHY (Fenske *et al.*, 2015), as well as by MYB family TFs such as ODO1 (Boersma *et al.*, 2022) and EOBs (Spitzer-Rimon *et al.*, 2012).

Chromatin regulation, including histone modification, DNA methylation, and nucleosome positioning, alters the accessibility of gene loci to transcription machinery and affects gene expression (Gendrel & Colot, 2005; Yuan *et al.*, 2013). Specifically, histone acetylation promotes active gene expression by increasing DNA accessibility and facilitating recruitment of transcription machinery (Xu *et al.*, 2005; Malapeira *et al.*, 2012). To date, our understanding of the role of chromatin level regulation in the temporal control of specialized metabolism is still at its infancy (Zhang *et al.*, 2016). Recently, chromatin level regulation, especially histone acetylation, was shown to regulate the floral VOC metabolic network during flower development (Patrick *et al.*, 2021). Chromatin level control was implicated in maintaining the central circadian clock (Malapeira *et al.*, 2012), however, little is known about the direct involvement of chromatin level regulation in the rhythmic control of specialized metabolism. In this study, using petunia (*P. hybrida* cv Mitchell) flowers that emit high levels of Phe-derived VOCs as a model system and time-course chromatin immunoprecipitation (ChIP) of histone modifications as the main approach, we show that rhythmic H3K9ac and H3K27ac are associated with specific genes in the floral VOC metabolic network, which exhibit a strong day–night oscillation in their transcript levels. Intriguingly, analysis of the dynamics of histone acetylation revealed a specific loss of histone acetylation marks at night, possibly to shut down the carbon flow into the specialized metabolic network, thus downregulating the biosynthesis of floral volatile compounds during the daytime when they are not needed.

Materials and Methods

Plant materials

Petunia hybrida cv. Mitchell plants were grown under standard glasshouse conditions at the Purdue University Horticulture Plant Growth Facility. Plants were maintained under a 14-h light period (6:00 h to 20:00 h).

Petunia corolla ChIP

Corolla tissue was harvested from Day 2 petunia flowers for ChIP in six samples taken 4 h apart, from 07:00 h to 03:00 h, with 20 flowers (*c.* 3.2 g) used per replicate. Corolla tissue was crosslinked under vacuum in 1% formaldehyde twice for 10 min and the reaction was stopped with the addition of 2 M glycine under vacuum for 5 min. The tissue was washed three times with ultrapure water, dried, flash frozen in liquid nitrogen, and then ground. Chromatin extraction and immunoprecipitation were performed as described previously (Patrick *et al.*, 2021). The antibodies used were α-H3K4me3 (07-473; Millipore Sigma, Burlington, MA, USA), α-H3K9ac (07-352; Millipore Sigma), α-H3K27ac (07-360; Millipore Sigma), and α-H3K36me3 (ab9050; Abcam). Input and ChIP sample concentrations were determined by Qubit dsDNA HS assay (Invitrogen).

ChIP-Seq and data analysis

Input and ChIP samples from 07:00 h to 19:00 h were used for library construction as previously described (Patrick *et al.*, 2021) using NEBNext Multiplex Oligos (New England Biolabs, Ipswich, MA, USA). Libraries were pooled and sequenced by Novogene (Sacramento, CA, USA) (Illlumina NovaSeq 6000 platform, paired-end, 2 × 150 bp). ChIP-Seq analysis was performed similarly to previously described (Patrick *et al.*, 2021). Adaptors were trimmed with CUTADAPT (v.1.13; Martin, 2011), and reads were aligned to the *Petunia axillaris* (v.1.6.2) and *P. inflata* (v.1.0.1) genomes (Bombarely *et al.*, 2016) with BOWTIE 2 (v.2.3.3.1; Langmead & Salzberg, 2012). Properly paired aligned reads were converted to a fragment bed format using BEDTOOLS (v.2.27.1; Quinlan & Hall, 2010). Pearson correlation of genic ChIP-Seq signals between replicates at the same time point for the same mark showed high agreement between replicates (Fig. S1), and positional plots of ChIP-Seq signals indicate effective immunoprecipitation and data analysis (Fig. S2). The aligned fragments were used to determine differentially present islands at 07:00 h and 19:00 h using SICER v.1.1 (Zang *et al.*, 2009) with an FDR cutoff of < 0.01 for significance (SICER-df.sh with gap size = 200, window size = 200, and effective genome size = 0.9), for two biological replicates for each histone mark with corresponding input DNA as background. Significant islands with ≥ 2-fold change between the two timepoints were retained and peaks present in both replicates were intersected to determine significantly phased islands at 07:00 h and 19:00 h. Significantly phased islands were intersected with *P. axillaris* gene features to determine phased DMGs as using bedtools 'closest' function.

RNA-Seq and data analysis

Total RNA was extracted from corolla tissue at 07:00 h and 19:00 h timepoints as described previously (Klempien *et al.*, 2012). Poly(A) enrichment, library preparation, and sequencing were performed by the Purdue Genomics Core Facility (Illumina HiSeq 2500 platform, paired-end, 2 × 100 bp). Differentially expressed genes (DEGs) were determined similarly to previously described (Patrick *et al.*, 2021). Briefly, reads were trimmed using CUTADAPT (v.1.13; Martin, 2011) and aligned to the *Petunia axillaris* (v.1.6.2) and *P. inflata* (v.1.0.1) genomes (Bombarely *et al.*, 2016) with TOPHAT2 (v.2.1.1; Kim *et al.*, 2013). Aligned reads in *P. axillaris* gene features were quantified with HTSEQ (v.0.7.0; Anders *et al.*, 2015); DEGs were

determined using DESeq2 (v.1.24.0) with a fold change cutoff of > 2 at 19:00 h relative to 07:00 h or vice versa with an FDR < 0.05. The quality of replication was additionally verified by principal component analysis (Fig. S3).

Functional enrichment analysis

Gene Ontology (GO) term enrichment in gene lists generated by ChIP-Seq and RNA-Seq analysis was performed in a *P. axillaris* background using an in-house Python script as previously described (Patrick *et al.*, 2021). Petunia metabolic pathway gene analysis was performed using previously annotated petunia VOC and SAM pathway gene lists (Patrick *et al.*, 2021; Boersma *et al.*, 2022).

ChIP-qPCR

ChIP-qPCR was performed using PowerUp SYBR (Applied Biosystems, Foster City, CA, USA) reagent with primers designed against predicted peak regions using Primer3 (Untergasser *et al.*, 2007) or with previously described primers (Patrick *et al.*, 2021; Table S1). Signal for each gene was determined relative to input and then, normalized against signal at two housekeeping control genes, *UBC9* and *ACTIN*.

Inhibitor assays

Histone acetyltransferase inhibitor assays were performed similarly to previously described (Patrick *et al.*, 2021). Briefly, Day 2 flowers were floated in a 3% sucrose solution and treated with MB-3 (Millipore Sigma) at a final concentration of 100 μM in 0.1% DMSO, or mock treatment (0.1% DMSO). Corolla samples were harvested at 4-h time points starting at 07:00 h, through 23:00 h. RNA was extracted from corolla samples using RNeasy Plant Mini Kit (Qiagen), followed by treatment with recombinant RNase-free DNase I (Roche) at 37°C for 1 h. Total RNA was then recovered by clean-up with the RNeasy Mini Kit (Qiagen).

qRT-PCR

cDNA was generated using SuperScript IV (Invitrogen) with an oligo(dT) primer. qRT-PCR was performed using PowerUp SYBR (Applied Biosystems) reagent with primers designed using Primer3 (Untergasser *et al.*, 2007) or with previously described primers (Adebesin *et al.*, 2017; Patrick *et al.*, 2021; Boersma *et al.*, 2022; Table S1). Gene expression was normalized to two control genes, *FBP1* and *UBQ10*.

Results

Dynamic histone acetylation, but not histone methylation, is observed for evening-phased floral VOC genes

Petunia flowers (*P. hybrida* cv Mitchell) emit floral VOCs from the corolla tissues in an oscillating manner during daily light–dark cycles (Fig. 1a; Kolosova *et al.*, 2001). The highest levels of emission were found around midnight, the time of the day when the moth pollinator are most active (Kolosova *et al.*, 2001; Fig. 1a). Consistent with this, gene expression and enzyme activities required for the biosynthesis and emission of petunia floral VOCs often reach their peak around later afternoon and early evening (Kolosova *et al.*, 2001). We hypothesized that dynamic and reversable chromatin level regulation participates in directing oscillation of the floral VOC metabolic network, promoting active transcription of the VOC genes during the evening while repressing gene expression in the morning. To test this hypothesis, corolla tissues of petunia plants grown under standard glasshouse conditions (light period: 06:00 h–20:00 h) were harvested for histone ChIP sequencing (ChIP-Seq). Corolla tissues were harvested at two time points, 07:00 h and 19:00 h on the second day after anthesis, representing the daily lowest and highest VOC gene expression, respectively (Fig. 1a). As activation of VOC pathway genes in the evening was particularly of interest, histone marks associated with transcriptional activation, H3K9ac, H3K27ac, H3K4me3, and H3K36me3, were chosen as the focus of this study (Jenuwein, 2001; He *et al.*, 2011). Genes associated with significantly increased levels of histone modification at 19:00 h relative to 07:00 h were determined (FDR < 0.01, fold change [FC] ≥ 2 in two biological replicates) and referred to as *evening-phased differentially modified genes* (*DMGs*). By contrast, genes associated with significantly increased histone modification at 07:00 h relative to 19:00 h were referred to as *morning-phased DMGs*.

Overall, a widespread reprogramming of histone modifications was observed in the petunia genome from the morning to evening. Across the four histone marks assayed, more genomic regions exhibited morning-phased histone modification (in the number of thousands) than the genomic regions showing evening-phased histone modification (in the number of hundreds; Fig. S4). On average, *c.* 49% of the dynamic genomic regions are located to annotated genes (Fig. S4). The morning-phased DMGs are largely enriched in biological processes such as circadian rhythm, photoprotection, and response to light and heat (Dataset S1a–d; Fig. S5). Since the floral scent pathways are activated toward the evening, we focused on analyzing the genes that gain activation marks at 19:00 h (Dataset S1e–h). Among the four analyzed activation marks, H3K9ac is increased at 269 genes and H3K27ac is increased at 224 genes at 19:00 h; by contrast, H3K4me3 and H3K36me3 are increased respectively at eight genes and three genes only (Fig. 1b). Thus, our results suggest an active deposition of histone acetylation marks, rather than histone methylation, toward the evening.

Notably, DMGs with evening-phased H3K9ac and those with evening-phased H3K27ac exhibit a substantial overlap (105/224) and are enriched with biological processes 'aromatic amino acid biosynthesis' and 'phenylpropanoid metabolism' (Fig. 1c,d). This suggests that these two permissive marks are associated with metabolic pathways contributing to the synthesis of precursors (Phe) and phenylpropanoid compounds for floral VOCs. As further support, there are significant overlaps between the

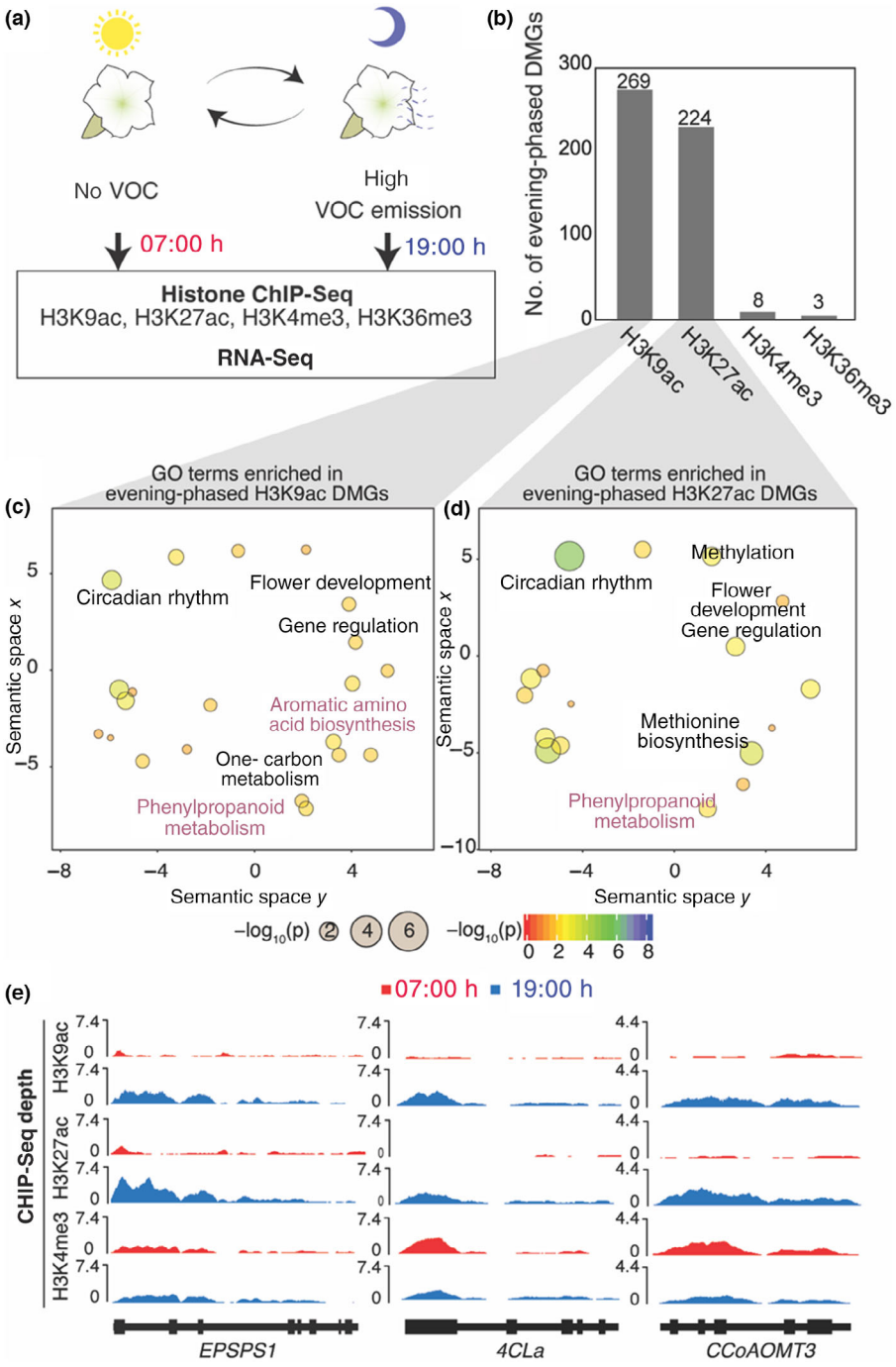

Fig. 1 Evening-phased histone acetylation in petunia corolla. (a) Petunia corolla tissue, exhibiting a scent emission peak in the evening, was harvested at 07:00 h and 19:00 h to analyze genome-wide histone modifications and gene expression. (b) Hundreds of genes are found to show higher level of histone acetylation (H3K9ac and H3K27ac) in the 19:00 h samples compared with the 07:00 h samples. Significant Gene Ontology (GO) terms enriched among differentially modified genes (DMGs) with increased H3K9ac (c) or increased H3K27ac (d) at 19:00 h vs 07:00 h in petunia corolla are shown in sematic spaces generated by REVIGO. Each circle in the sematic space represents a significant GO term, and the size and color of the circle represent the level of significance of the enrichment. (e) Histone ChIP-Seq coverage showing dynamic H3K9ac and H3K27ac deposition along gene body of VOC genes from 07:00 h to 19:00 h. By contrast, H3K4me3 remains stable. The sequencing depth was scaled to library size. Representative results from one of two independent biological replicates are shown. 4CL, 4-coumaryl-CoA ligase; EPSPS, 5-*enol*pyruvylshikimate 3-phosphate synthase; CCoAOMT3, caffeoyl-CoA O-methyltransferase; VOC, volatile organic compound.

evening-phased H3K9ac or H3K27ac DMGs and the genes previously curated as involved in the floral VOC networks (Fig. S6A; Patrick *et al.*, 2021). Specifically, a significant increase in H3K9ac and H3K27ac levels was observed from 07:00 h to 19:00 h at gene loci involved in synthesizing the precursor phenylalanine and phenylalanine derivatives for VOC formation (Fig. 1e: *EPSPS1* and *4CLa*), as well as involved in the synthesis of monolignol precursors for the formation of volatile phenylpropenes (Fig. 1e: *CCoAOMT3*). By contrast, the H3K4me3 level at these gene loci shows little change between 07:00 h and 19:00 h (Fig. 1e).

Evening-phased histone acetylation at VOC-relevant gene loci are related to a strong oscillation in their mRNA levels

To understand the effect of observed dynamic histone modification patterns on global gene expression, RNA-Seq data were generated and analyzed from the same tissue and time points as the histone ChIP-Seq. We found a global reprogramming of gene expression in the corolla from 07:00 h to 19:00 h, including 2728 morning-phased DEGs (FC of 07:00 h/19:00 h > twofold; FDR < 0.05) and 2722 evening-phased genes (FC of 19:00 h/07:00 h > 2-fold; FDR < 0.05; Dataset S2). Not surprisingly, the

evening-phased DEGs, but not the morning-phased DEGs, are enriched with the genes involved in the VOC biosynthesis and emission pathways (Fig. S7A). The evening-phased DEGs are significantly overrepresented with many GO terms relevant to the production of floral VOCs, including 'aromatic amino acid biosynthesis' for providing the precursor Phe, 'phenylpropanoid biosynthesis' for the formation of VOCs, and 'S-adenosylmethionine biosynthesis' and 'one-carbon metabolism' that potentially contribute the methyl groups for the production of volatile metabolites such as methyl benzoate, eugenol, and isoeugenol (Patrick *et al.*, 2021; Boersma *et al.*, 2022; Fig. S8). Interestingly, genes involved in distinct steps of the floral VOCs biosynthetic pathways exhibit different magnitudes of oscillation of transcript levels, with the genes associated with the formation of volatile benzenoids displaying the lowest level of diurnal oscillation while the genes involved in the shikimate pathway, which provide the precursor for production of Phe, show the highest oscillation amplitudes (Fig. 2; Dataset S3).

To investigate the extent to which changes in histone modifications at a gene locus co-occur with changes in transcript levels, we compared the evening-phased DMGs and DEGs. As expected, a significant overlap was observed between the evening-phased DEGs and DMGs that gained H3K9ac or H3K27ac at 19:00 h (Fig. S7B). Interestingly, the evening-phased DEGs with a greater magnitude of oscillation (measured by FC of expression levels of 19:00 h in relation to 07:00 h) are more likely to be associated with evening-phased histone acetylation (Fig. 2).

The strongest oscillators are distinguished by a loss of histone acetylation in the morning

To investigate the observation that dynamic histone acetylation is more likely to be associated with the DEGs displaying a strong mRNA level oscillation (FC of mRNA levels at 19:00 h/07:00 h > 32, referred to as *strongest oscillators*; Fig. 2; Dataset S4a), and to a lesser extent with the DEGs showing mild oscillation (4 < FC < 32, referred to as *modest oscillators*; Fig. 2; Dataset S4b), the H3K9ac and H3K27ac levels were plotted across gene features for all the genes involved in the VOC biosynthesis and emission network, together with their mRNA level FC between 07:00 h and 19:00 h (Figs 3a, S9A). We initially hypothesized that the strongest oscillators would acquire higher levels of histone acetylation at 19:00 h, compared with the modest oscillators. Surprisingly, at 19:00 h, the strongest oscillators and the modest oscillators have comparable levels of H3K9ac and H3K27ac (Figs 3a, S9A). By contrast, the two groups of genes display drastically different histone acetylation levels at 07:00 h (Figs 3a, S9A). The strongest oscillators lose histone acetylation marks at 07:00 h, while the modest oscillators generally maintain their histone acetylation at 07:00 h (Figs 3a, S9A). The strongest oscillators include multiple genes encoding enzymes involved in the biosynthesis of Phe precursor, and genes encoding enzymes generating the metabolic intermediates in the phenylpropanoid pathways, in addition to a TF and a transporter (Dataset S4a; Fig. S10). The changes in

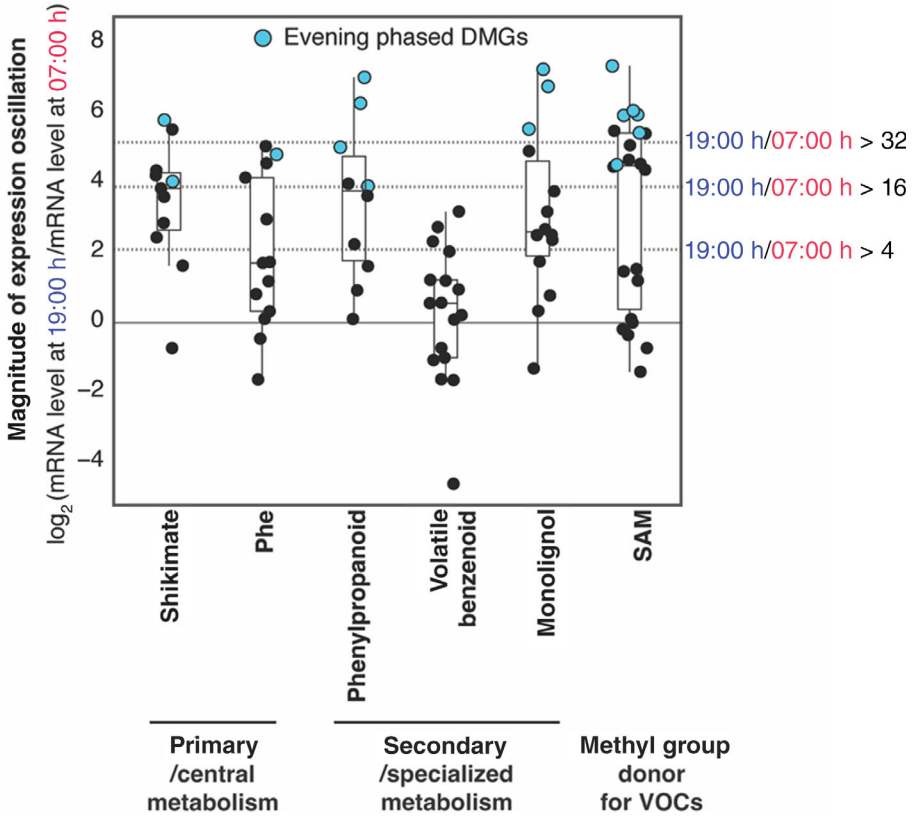

Fig. 2 Fold change in expression of floral VOC genes and association with evening-phased histone acetylation. Each circle represents a gene belonging to a specific subgroup of the floral VOC metabolic network (labeled in *x*-axis, see Supporting Information Dataset S3 for details). Floral VOC genes with a higher fold change in expression levels of 19:00 h relative to 07:00 h (*y*-axis) are more likely to be associated with evening-phased histone acetylation (represented by blue circles). DMG, differentially modified gene; Phe, phenylalanine; SAM, S-adenosylmethionine; VOC, volatile organic compound. Box plots show the second and third quartile of data, with a horizontal line at the median, while whiskers depict the range minus outliers. All data points are shown.

histone acetylation levels for the strongest oscillators are concentrated in the coding region, especially the first half (Figs 3a, S9A). By contrast, H3K4me3 and H3K36me3 show little dynamic changes at VOC pathway genes between 07:00 h and 19:00 h (Fig. S9B,C). Overall, we observed that the strongest oscillators were differentiated from the modest oscillators by loss of histone acetylation in the morning, rather than an increase in histone acetylation in the evening.

To attain further temporal resolution of the dynamics of histone acetylation, histone modifications and gene expression were analyzed in petunia corolla tissues at six time points during a 24-h day : night cycle, 07:00 h, 11:00 h, 15:00 h, 19:00 h, 23:00 h, and 03:00 h, with the light period from 06:00 h till 20:00 h. For the *strongest oscillators*, a robust induction of histone acetylation was observed from 11:00 h to 19:00 h (Figs 3b, S11A), likely reflecting the activity of histone acetyltransferase(s) during this specific period of the day. The histone acetylation peaks *c.* 19:00 h is followed by a drastic drop by 23:00 h (*c.* fivefold; Figs 3b, S11A), likely due to the activity of histone deacetylase(s). The dramatic reduction in histone acetylation after the evening peak leads to a low level of histone acetylation in the morning (e.g., 07:00 h; Figs 3b, S11A), which corresponds to a significant decrease in gene expression in the morning (Fig. 3c). This pattern was observed for the *strongest oscillators*, including genes encoding enzymes that synthesize Phe precursor and intermediates for the VOC synthesis (*EPSPS1*, *4CLa*, and *CCoAOMT3*; Dudareva *et al.*, 2013), as well as for the master TF regulator of floral VOC formation (*ODO1*; Boersma *et al.*, 2022) and the transporter involved in the emission of VOCs (*ABCG1*; Adebesin *et al.*, 2017). By contrast, despite the existence of a clear oscillation in mRNA levels (Fig. 3c), histone acetylation marks in the *modest oscillators* are relatively stable during the day–night cycle, particularly due to the high level of histone acetylation at 07:00 h (Fig. 3b). In agreement with this, the modest oscillators are expressed to a higher degree at 07:00 h than the strongest oscillators (Fig. 3c). Conversely, the histone methylation marks H3K4me3 and H3K36me3, despite often being linked to active gene transcription, remain stable through the day–night cycle for both strongest oscillators and modest oscillators (Fig. S11B,C).

Histone acetylation has a causal effect on the evening induction of VOC genes

Based on the distinct histone acetylation patterns of the strongest oscillators vs modest oscillators (Fig. 3a,b), we hypothesized that histone acetyltransferase(s) actively deposit histone acetylation marks on the strongest oscillator VOC genes from 07:00 h to 19:00 h, with a peak of activity between 11:00 h and 19:00 h (Figs. 3b, S11A), to increase their expression. We then attempted to determine whether inhibiting the histone acetyltransferase activity affects the evening induction of these VOC genes, and whether such effect is more pronounced for the strongest oscillators (which generally lack histone acetylation in the morning) relative to the modest oscillators. To do this, petunia flowers were treated with chemical inhibitor MB-3 to disrupt the daytime deposition of histone acetylation, and expression levels of both the strongest oscillator and modest oscillator VOC genes were measured using time-course qRT-PCR from 07:00 h to 19:00 h. The strong oscillators, including the regulator *ODO1* (Fig. 4a), transporter *ABCG1* (Fig. 4b), as well as biosynthetic enzymes *4CLa* (Fig. 4c) and *CCoAOMT3* (Fig. 4d), exhibited significant reduction in their evening induction (measured as FC of gene expression at 11:00 h, 15:00 h, and 19:00 h relative to 07:00 h) when treated with MB-3. By contrast, the effect on the induction of modest oscillator genes was less pronounced (Fig. 4e,f).

Discussion

Our integrated analysis of epigenomic and transcriptomic data revealed that in a rhythmically regulated specialized metabolic pathway, genes demonstrating the most dramatic oscillation of transcript level during the day–night cycle are associated with highly dynamic histone acetylation changes from morning to evening (Fig. 2). Our data support a model wherein H3K9/K27 acetylation is deposited in the early afternoon to promote high levels of transcription of the relevant genes in the evening, thereby enabling the release of floral scents around midnight when the pollinator moth is most active (Fig. 4g). At night, the histone acetylation marks are erased, in coordination with a

Fig. 3 Strongest oscillating genes involved in the floral volatile pathways are associated with distinct H3K9ac removal in the morning. (a) Each row represents one gene involved in the biosynthesis and emission of floral scents, and the mRNA level change in the genes between 19:00 h and 07:00 h was plotted as a single column heatmap on the right. Genes showing the strongest induction from 07:00 h to 19:00 h (fold change > 32) are ranked on the top and represented by dark turquoise color, referred to as strongest oscillators. Genes showing an induction fold change between 4 and 32 are referred to as modest oscillators. The H3K9ac level determined by ChIP-Seq was plotted along the gene feature from 1 kb upstream to 1-kb downstream, where the red represents high level of H3K9ac and the yellow represents low level of H3K9ac, for samples harvested at 07:00 h and 19:00 h separately. The difference in H3K9ac levels between 19:00 h and 07:00 h is also plotted as heatmap along gene features, where green represents increase in H3K9ac at 19:00 h compared with 07:00 h, and hot pink represents decrease in H3K9ac at 19:00 h compared with 07:00 h. The results show that the strongest oscillators are associated with the most dramatic H3K9ac level changes during the day–night cycle, featuring a distinct loss of H3K9ac during the morning, compared with genes that oscillate with more modest transcript level changes during the day–night cycle. (b, c) Time-course ChIP-qPCR ($n = 3$) and qRT-PCR ($n = 4$) show that the H3K9ac dramatically increases from 11:00 h to 15:00 h and then rapidly decreases from 19:00 h to 23:00 h, at genes with strong transcript level oscillation (*ODO1*, *ABCG1*, *EPSPS1*, *4CLa*, and *CCoAOMT3*); by contrast, genes with modest transcript oscillation (*ADT1* and *PALc*) are associated with mild changes in histone acetylation and do not display histone acetylation removal during the night. Error bars represent standard error of the mean. 4CL, 4-coumaryl-CoA ligase; EPSPS, 5-*enol*pyruvylshikimate 3-phosphate synthase; CCoAOMT3, caffeoyl-CoA O-methyltransferase; PAL, phenylalanine ammonia lyase; VOC, volatile organic compound.

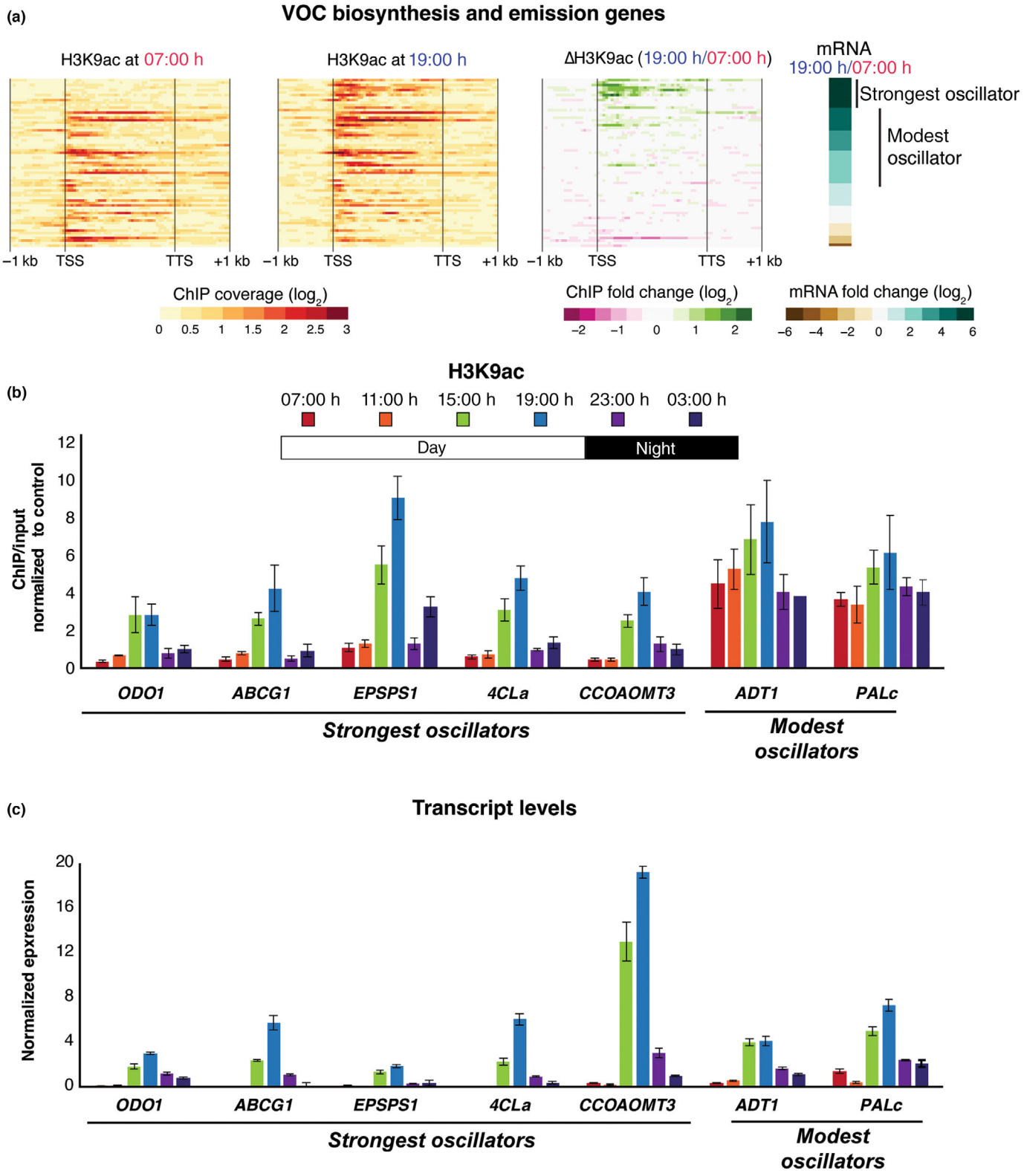

drastic decrease in transcriptional activity of the corresponding genes in the morning when the pollinators are not present (Fig. 4g). Interestingly, genes in the VOC network that are most dynamically regulated are distinguished from the rest by a lower level of histone acetylation when their activity is not desired, rather than a higher peak level of histone acetylation when their

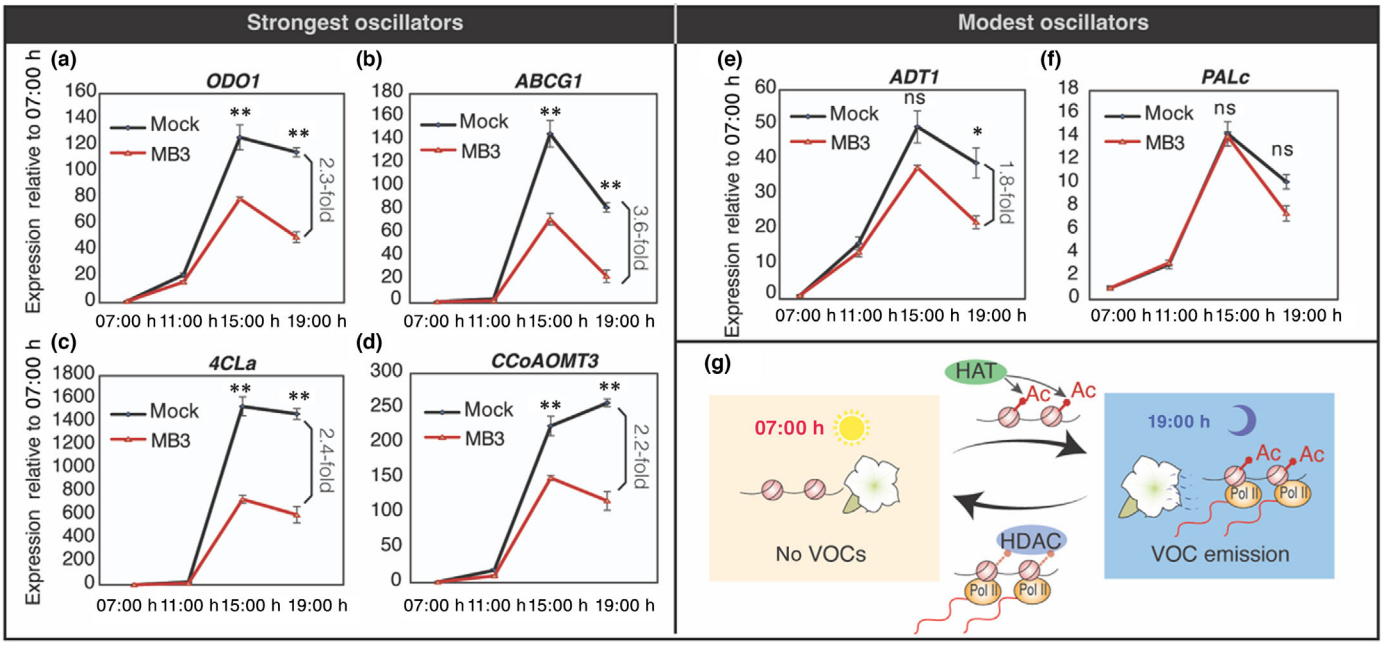

Fig. 4 Chemical inhibition of histone acetylation affects evening induction of VOC genes. (a) qRT-PCR showing that the induction of VOC genes in the afternoon and evening is impaired by histone acetyltransferase inhibitor MB-3. Error bars represent standard error of the mean for biological replicates ($n = 4$–6). Statistical significance of differences between the mock and treatment expression levels were determined using Student's *t*-test. The *P*-value of the significant difference is indicated by asterisks: (*, $P < 0.05$; **, $P < 0.01$; ns, not significant). Specifically, inhibition of histone acetylation significantly compromises the evening induction of strong oscillators (a–d), but with less or no effect on the modest oscillators (e, f). This result, in combination with others, supports a model (g) wherein H3K9/K27 acetylation is deposited in the early afternoon to promote high levels of transcription of the relevant genes in the evening. At night, the histone acetylation marks are erased, possibly leading to a drastic decrease in transcriptional activity of the corresponding genes in the morning, when pollinators are not present. 4CL, 4-coumaryl-CoA ligase; EPSPS, 5-*enol*pyruvylshikimate 3-phosphate synthase; CCoAOMT3, caffeoyl-CoA O-methyltransferase; HAT, histone acetyltransferase; HDAC, histone deacetylase; PAL, phenylalanine ammonia lyase; VOC, volatile organic compound.

activity is required (Fig. 3a). The apparent importance of this deactivation of the specialized metabolic pathway likely reflects the need to maintain the balance between central and specialized metabolism, with the latter consuming carbon and energy from the former. Therefore, in the absence of pollinator activity, when the volatile specialized metabolites are not required, it is likely that key genes involved in the biosynthetic pathways are deactivated through the abrogation of the histone acetylation mark, thus ensuring that no leaking gene expression occurs and resource are not 'trickled' into the specialized metabolic pathways and lost to the atmosphere. By contrast, the histone methylation marks we assayed, H3K4me3 and H3K36me3, are less dynamic during the day–night cycle (Fig. S11). Therefore, although they are all considered as marks associated with active gene transcription, different histone marks (e.g. H3K9/27ac vs H3K4/36me3) might have distinct roles in how they specifically affect the gene transcription process, in that one mark might poise the gene generally permissive for transcription depending on specific tissue and developmental context, while the other mark might fine-tune the transcriptional activity based on environmental inputs.

It is intriguing to investigate the logic and mechanisms that determine genes exhibiting the strongest oscillations (i.e. greater fold change in gene expression and dynamic histone acetylation, with a more complete loss of histone acetylation in the morning), vs modest oscillators (i.e. smaller fold change in gene expression, and much less dynamic histone acetylation with a substantial level of histone acetylation in the 'off' phase). Our results show that the strongest oscillators include the following four categories (Dataset S4a; Fig. S10): (1) master regulator of the floral VOC network – the key TF *ODO1* (Boersma *et al.*, 2022); (2) genes involved in driving the synthesis of primary metabolite precursor for VOC synthesis (e.g. *EPSPS1*; Fig. S10A); (3) genes encoding enzymes catalyzing metabolic conversions close to the branching points of metabolic pathways, possibly to direct carbon into producing floral VOCs, such as *C4H*, *4CLa*, and *CCoAOMT3* (Fig. S10B); and (4) gene encoding a transporter facilitating the mass transfer across the plasma membrane and subsequent release of volatiles into the atmosphere (*ABCG1*; Adebesin *et al.*, 2017). The overall logic of regulation seems to focus on a systems-level control of the network as well as modulation of carbon flux toward floral VOC production through tuning the level of precursor Phe and intermediate metabolites in the branching pathways. The end-step enzymes are in general absent in the list of strongest oscillators, in agreement with the notion that the pathway activity is largely driven by the availability of substrates (Colquhoun *et al.*, 2010; Maeda *et al.*, 2010). An exception was *ABCG1*, which is involved in the VOC emission – the active transport of VOCs across plasma membrane for release into the atmosphere (Adebesin *et al.*, 2017). It is intriguing why the end-step transporter *ABCG1* is highly regulated, with gene transcription strongly reduced during the off phase, distinctly different from the end-step enzymes. One possible explanation is that the

reduction in ABCG1-mediated transport activity will result in a moderate accumulation of residual VOCs inside the cell, which then triggers feedback regulation to further inhibit the enzymatic activity of the VOC pathways through allosteric inhibition. The accumulation of internal volatile compounds can also further down-regulate the transcript level of many VOC biosynthetic genes through unknown mechanisms (Liao *et al.*, 2021). In other words, down-regulation of *ABCG1* likely strengthens the suppression of the pathways by inducing metabolite-mediated feedback inhibition. Another possibility is that ABCG1 may also transport other metabolites in a nonspecific manner; therefore, reducing its expression prevents the plant cell from losing carbon resources due to the residual activity of this transporter.

How is such target specificity achieved? The answer might lie in the histone acetyltransferases (HATs) and histone deacetylases (HDACs) responsible for this dynamic histone acetylation pattern. We showed that MB-3 could significantly inhibit the evening induction of the strongest oscillators (Fig. 4). MB-3 is capable of inhibiting both the p300/CBP and GNAT/MYST family of HATs (Biel *et al.*, 2004; Bowers *et al.*, 2010). Our results thus suggest that unknown member(s) of the p300/CBP or GNAT/MYST families of HATs likely contribute to the transcriptional activation of VOC biosynthesis from 11:00 h to 19:00 h (Fig. 3). Similarly, an unknown HDAC removes the histone acetylation from 19:00 h to 23:00 h (Fig. 3). The identification of this HAT-HDAC pair is the focus of the next step of investigation. Dynamic histone acetylation is observed in gene body, mostly the first few exons of the gene (Fig. 3), rather than the promoters. Therefore, these HAT-HDACs are likely associated with the initiation phase of the transcription elongation process. How do the HAT-HDAC pair recognize their target genes in the genome? While some histone-modifying enzymes are known to bind nucleotide motifs for target specificity (Cui *et al.*, 2016; Wang *et al.*, 2017), HATs and HDACs are likely to be recruited to their target genes by interacting with TFs (Weiste & Dröge-Laser, 2014). ODO1 is a possible candidate TF for recruiting HATs and HDACs to target genes in the floral VOC pathway, since it regulates many genes in the floral VOC network (Boersma *et al.*, 2022) and is itself regulated by the plant circadian clock, with expression peaking in the evening (Fenske *et al.*, 2015). Indeed, there is a significant overlap between genes known to be ODO1 binding targets (Boersma *et al.*, 2022) and the strongest oscillators. However, a significant overlap also exists between ODO1-bound genes and those which exhibit modest oscillation and lack dynamic histone acetylation. In agreement with this, the promoters of both strong oscillators and modest oscillators are enriched with a MYB binding motif, as determined by MEME (Bailey & Elkan, 1994), that is highly similar to the binding motif for ODO1 (Boersma *et al.*, 2022; Fig. S12). Therefore, it is unlikely that ODO1 is solely responsible for recruiting HATs and HDACs to the strongest oscillators.

Recent studies have shown that the floral VOC pathways are controlled by circadian clock (Fenske *et al.*, 2015). In addition to the traditional model of TF proteins controlling the circadian clock, chromatin modifications have been increasingly identified as a regulatory layer in modulating the clock. Reversible and dynamic histone modifications have been shown to oscillate at circadian clock gene loci and play an essential role in maintaining the precise phase of the clock in both plants and mammals (Perales & Más, 2007; Malapeira *et al.*, 2012; Papazyan *et al.*, 2016). It was unclear, however, whether genes operating under the control of the clock (e.g. VOC pathways) are also associated with rhythmic chromatin modifications, and, if so, whether they employ the same or distinct mechanisms from those of the clock genes (Trott & Menet, 2018). Our ChIP analyses from petunia flowers reveal that metabolic pathways controlled by circadian clock are directly regulated by oscillating histone acetylation, and likely through different mechanisms. Indeed, the positional profile of histone acetylation differs between metabolic pathway genes and the evening clock genes: in comparison to VOC genes, whose dynamic histone acetylation often begins in the gene body where transcriptional elongation occurs (Fig. 3), many clock genes display dynamic histone acetylation around the promoter and transcription start site (Fig. S13). Moreover, the histone methylation marks such as H3K4me3 oscillate at circadian clock genes (Malapeira *et al.*, 2012), but not at the strongly oscillating VOC genes (Fig. S11B), further indicating different mode-of-action for epigenetic control of circadian clock vs gene networks controlled by circadian clock. The oscillating histone acetylation marks at VOC genes could be controlled by circadian clock proteins, either directly or indirectly. Alternatively, the machinery involved in establishing daily dynamic histone acetylation patterns at VOC genes might be regulated by light/dark transition rather than the circadian clock, a scenario that needs future investigation.

Acknowledgements

This research is supported by the National Science Foundation grants MCB-2123470 to YL and ND, and a seed grant to YL and ND from the Purdue Center for Plant Biology, USDA National Institute of Food and Agriculture Hatch project numbers 1013620 to YL, 177845 to ND, and an Agriculture and Food Research Initiative Postdoctoral Fellowship (grant no. 2019-67012-29660) to RMP from the USDA National Institute of Food and Agriculture. We thank Antje Klempien for isolating RNA for the generation of RNA-Seq datasets.

Competing interests

None declared.

Author contributions

RMP, YL and ND conceived and designed the study. RMP and X-QH. performed the experiments and data analysis. RMP, X-QH, YL and ND wrote and revised the manuscript.

ORCID

Natalia Dudareva https://orcid.org/0000-0003-0777-7763
Xing-Qi Huang https://orcid.org/0000-0002-9402-7735

Ying Li https://orcid.org/0000-0002-5258-7355
Ryan M. Patrick https://orcid.org/0000-0003-2396-0680

Data availability

RNA-Seq data generated in this work are available at the NCBI Gene Expression Omnibus (GEO) Database under accession no. GSE230802. ChIP-Seq data generated in this work are available at the NCBI GEO Database under accession GSE230857.

References

Adebesin F, Widhalm JR, Boachon B, Lefevre F, Pierman B, Lynch JH, Alam I, Junqueira B, Benke R, Ray S *et al.* 2017. Emission of volatile organic compounds from petunia flowers is facilitated by an ABC transporter. *Science* **356**: 1386–1388.

Anders S, Pyl PT, Huber W. 2015. HTSeq–a Python framework to work with high-throughput sequencing data. *Bioinformatics* **31**: 166–169.

Bailey TL, Elkan C. 1994. Fitting a mixture model by expectation maximization to discover motifs in biopolymers. In: *Proceedings of the Second International Conference on Intelligent Systems for Molecular Biology*. Menlo Park, CA, USA: AAAI Press, 28–36.

Biel M, Kretsovali A, Karatzali E, Papamatheakis J, Giannis A. 2004. Design, synthesis, and biological evaluation of a small-molecule inhibitor of the histone acetyltransferase Gcn5. *Angewandte Chemie* **43**: 3974–3976.

Boersma MR, Patrick RM, Jillings SL, Shaipulah NFM, Sun P, Haring MA, Dudareva N, Li Y, Schuurink RC. 2022. ODORANT1 targets multiple metabolic networks in petunia flowers. *The Plant Journal* **109**: 1134–1151.

Bombarely A, Moser M, Amrad A, Bao M, Bapaume L, Barry CS, Bliek M, Boersma MR, Borghi L, Bruggmann R *et al.* 2016. Insight into the evolution of the Solanaceae from the parental genomes of *Petunia hybrida*. *Nature Plants* **2**: 16074.

Bowers EM, Yan G, Mukherjee C, Orry A, Wang L, Holbert MA, Crump NT, Hazzalin CA, Liszczak G, Yuan H *et al.* 2010. Virtual ligand screening of the p300/CBP histone acetyltransferase: identification of a selective small molecule inhibitor. *Chemistry & Biology* **17**: 471–482.

Colquhoun TA, Verdonk JC, Schimmel BCJ, Tieman DM, Underwood BA, Clark DG. 2010. Petunia floral volatile benzenoid/phenylpropanoid genes are regulated in a similar manner. *Phytochemistry* **71**: 158–167.

Cui X, Lu F, Qiu Q, Zhou B, Gu L, Zhang S, Kang Y, Cui X, Ma X, Yao Q *et al.* 2016. REF6 recognizes a specific DNA sequence to demethylate H3K27me3 and regulate organ boundary formation in Arabidopsis. *Nature Genetics* **48**: 694–699.

Dudareva N, Murfitt LM, Mann CJ, Gorenstein N, Kolosova N, Kish CM, Bonham C, Wood K. 2000. Developmental regulation of methyl benzoate biosynthesis and emission in snapdragon flowers. *Plant Cell* **12**: 949–961.

Dudareva N, Klempien A, Muhlemann JK, Kaplan I. 2013. Biosynthesis, function and metabolic engineering of plant volatile organic compounds. *New Phytologist* **198**: 16–32.

Fenske MP, Hazelton KDH, Hempton AK, Shim JS, Yamamoto BM, Riffell JA, Imaizumi T. 2015. Circadian clock gene *LATE ELONGATED HYPOCOTYL* directly regulates the timing of floral scent emission in *Petunia*. *Proceedings of the National Academy of Sciences, USA* **112**: 9775–9780.

Gendrel A-V, Colot V. 2005. Arabidopsis epigenetics: when RNA meets chromatin. *Current Opinion in Plant Biology* **8**: 142–147.

He G, Elling AA, Deng XW. 2011. The epigenome and plant development. *Annual Review of Plant Biology* **62**: 411–435.

Holopainen JK, Gershenzon J. 2010. Multiple stress factors and the emission of plant VOCs. *Trends in Plant Science* **15**: 176–184.

Jenuwein T. 2001. Translating the histone code. *Science* **293**: 1074–1080.

Kim D, Pertea G, Trapnell C, Pimentel H, Kelley R, Salzberg SL. 2013. TopHat2: accurate alignment of transcriptomes in the presence of insertions, deletions and gene fusions. *Genome Biology* **14**: R36.

Klee HJ. 2010. Improving the flavor of fresh fruits: genomics, biochemistry, and biotechnology. *New Phytologist* **187**: 44–56.

Klempien A, Kaminaga Y, Qualley A, Nagegowda DA, Widhalm JR, Orlova I, Shasany AK, Taguchi G, Kish CM, Cooper BR *et al.* 2012. Contribution of CoA ligases to benzenoid biosynthesis in petunia flowers. *Plant Cell* **24**: 2015–2030.

Knudsen JT, Eriksson R, Gershenzon J, Ståhl B. 2006. Diversity and distribution of floral scent. *The Botanical Review; Interpreting Botanical Progress* **72**: 1–120.

Kolosova N, Gorenstein N, Kish CM, Dudareva N. 2001. Regulation of circadian methyl benzoate emission in diurnally and nocturnally emitting plants. *Plant Cell* **13**: 2333–2347.

Langmead B, Salzberg SL. 2012. Fast gapped-read alignment with Bowtie 2. *Nature Methods* **9**: 357–359.

Liao P, Ray S, Boachon B, Lynch JH, Deshpande A, McAdam S, Morgan JA, Dudareva N. 2021. Cuticle thickness affects dynamics of volatile emission from petunia flowers. *Nature Chemical Biology* **17**: 138–145.

Liao P, Maoz I, Shih M-L, Lee JH, Huang X-Q, Morgan JA, Dudareva N. 2023. Emission of floral volatiles is facilitated by cell-wall non-specific lipid transfer proteins. *Nature Communications* **14**: 330.

Maeda H, Shasany AK, Schnepp J, Orlova I, Taguchi G, Cooper BR, Rhodes D, Pichersky E, Dudareva N. 2010. RNAi suppression of Arogenate Dehydratase1 reveals that phenylalanine is synthesized predominantly via the arogenate pathway in petunia petals. *Plant Cell* **22**: 832–849.

Malapeira J, Khaitova LC, Mas P. 2012. Ordered changes in histone modifications at the core of the Arabidopsis circadian clock. *Proceedings of the National Academy of Sciences, USA* **109**: 21540–21545.

Martin M. 2011. Cutadapt removes adapter sequences from high-throughput sequencing reads. *EMBnet.Journal* **17**: 10.

Muhlemann JK, Maeda H, Chang C-Y, Miguel PS, Baxter I, Cooper B, Ann Perera M, Nikolau BJ, Vitek O, Morgan JA *et al.* 2012. Developmental changes in the metabolic network of snapdragon flowers. *PLoS ONE* **7**: e40381.

Papazyan R, Zhang Y, Lazar MA. 2016. Genetic and epigenomic mechanisms of mammalian circadian transcription. *Nature Structural & Molecular Biology* **23**: 1045–1052.

Patrick RM, Huang X-Q, Dudareva N, Li Y. 2021. Dynamic histone acetylation in floral volatile synthesis and emission in petunia flowers. *Journal of Experimental Botany* **72**: 3704–3722.

Perales M, Más P. 2007. A functional link between rhythmic changes in chromatin structure and the Arabidopsis biological clock. *Plant Cell* **19**: 2111–2123.

Quinlan AR, Hall IM. 2010. BEDTools: a flexible suite of utilities for comparing genomic features. *Bioinformatics* **26**: 841–842.

Schwab W, Davidovich-Rikanati R, Lewinsohn E. 2008. Biosynthesis of plant-derived flavor compounds. *The Plant Journal* **54**: 712–732.

Spitzer-Rimon B, Farhi M, Albo B, Cna'ani A, Zvi MMB, Masci T, Edelbaum O, Yu Y, Shklarman E, Ovadis M *et al.* 2012. The R2R3-MYB–like regulatory factor EOBI, acting downstream of EOBII, regulates scent production by activating ODO1 and structural scent-related genes in Petunia. *Plant Cell* **24**: 5089.

Trott AJ, Menet JS. 2018. Regulation of circadian clock transcriptional output by CLOCK:BMAL1. *PLoS Genetics* **14**: e1007156.

Untergasser A, Nijveen H, Rao X, Bisseling T, Geurts R, Leunissen JAM. 2007. Primer3Plus, an enhanced web interface to Primer3. *Nucleic Acids Research* **35**: W71–W74.

Verdonk JC, Ric de Vos CH, Verhoeven HA, Haring MA, van Tunen AJ, Schuurink RC. 2003. Regulation of floral scent production in petunia revealed by targeted metabolomics. *Phytochemistry* **62**: 997–1008.

Vickers CE, Gershenzon J, Lerdau MT, Loreto F. 2009. A unified mechanism of action for volatile isoprenoids in plant abiotic stress. *Nature Chemical Biology* **5**: 283–291.

Wang X, Paucek RD, Gooding AR, Brown ZZ, Ge EJ, Muir TW, Cech TR. 2017. Molecular analysis of PRC2 recruitment to DNA in chromatin and its inhibition by RNA. *Nature Structural & Molecular Biology* **24**: 1028–1038.

Weiste C, Dröge-Laser W. 2014. The Arabidopsis transcription factor bZIP11 activates auxin-mediated transcription by recruiting the histone acetylation machinery. *Nature Communications* **5**: 3883.

Xu C-R, Liu C, Wang Y-L, Li L-C, Chen W-Q, Xu Z-H, Bai S-N. 2005. Histone acetylation affects expression of cellular patterning genes in the Arabidopsis root epidermis. *Proceedings of the National Academy of Sciences, USA* **102**: 14469–14474.

Yuan L, Liu X, Luo M, Yang S, Wu K. 2013. Involvement of histone modifications in plant abiotic stress responses. *Journal of Integrative Plant Biology* **55**: 892–901.

Zang C, Schones DE, Zeng C, Cui K, Zhao K, Peng W. 2009. A clustering approach for identification of enriched domains from histone modification ChIP-Seq data. *Bioinformatics* **25**: 1952–1958.

Zhang B, Tieman DM, Jiao C, Xu Y, Chen K, Fei Z, Giovannoni JJ, Klee HJ. 2016. Chilling-induced tomato flavor loss is associated with altered volatile synthesis and transient changes in DNA methylation. *Proceedings of the National Academy of Sciences, USA* **113**: 12580–12585.

Supporting Information

Additional Supporting Information may be found online in the Supporting Information section at the end of the article.

Dataset S1 Genes with dynamic histone acetylations.

Dataset S2 Genes with dynamic expression levels.

Dataset S3 Metabolic pathway analysis (Related to Fig. 2).

Dataset S4 Genes classified as strongest or modest oscillators.

Fig. S1 Correlation between ChIP-Seq library replicates.

Fig. S2 Positional profile of ChIP-Seq coverage.

Fig. S3 Analysis of RNA-Seq replicates.

Fig. S4 Number of genomic regions (islands) identified as morning-phased (07:00 h > 19:00 h) (A) or evening-phased (19:00 h > 07:00 h) (B) for four histone modification marks assayed.

Fig. S5 Heatmap showing GO terms significantly enriched (adjusted $P < 0.05$) among the morning-phased DMGs.

Fig. S6 Intersections between DMGs with genes involved in the floral VOC pathways.

Fig. S7 Intersections between DEGs with genes involved in the floral VOC pathways.

Fig. S8 GO terms significantly enriched among evening-phased DEGs shown in sematic spaces generated by REVIGO.

Fig. S9 Heatmaps showing the histone modifications and gene expression level changes of floral VOC pathway genes at 07:00 h and 19:00 h.

Fig. S10 Primary metabolic network (A) and specialized metabolic network (B) contributing toward floral VOC formation.

Fig. S11 Time-course ChIP-qPCR.

Fig. S12 Significantly enriched promoter motifs among the 1 kb promoters of strong or modest oscillators.

Fig. S13 Heatmaps showing the histone acetylation and gene expression level changes of evening clock genes at 07:00 h and 19:00 h.

Table S1 Primers.

Please note: Wiley is not responsible for the content or functionality of any Supporting Information supplied by the authors. Any queries (other than missing material) should be directed to the *New Phytologist* Central Office.